

Salt isolation from waste brine enabled by interfacial solar evaporation with zero liquid discharge

Yida Wang¹, Xuan Wu^{1,*}, Pan Wu¹, Huimin Yu¹, Jingyuan Zhao¹, Xiaofei Yang², Qin Li³, Zhezi Zhang⁴, Dongke Zhang⁴, Gary Owens¹, and Haolan Xu^{1,*}

¹ Future Industries Institute, University of South Australia, Mawson Lakes Campus, Australia, SA 5095.

² College of Science, Nanjing Forestry University, Nanjing 210027, China.

³ Queensland Micro- and Nanotechnology Centre, Griffith University Nathan Campus, Brisbane, QLD 4111, Australia.

⁴ Centre for Energy (M473), The University of Western Australia, 35 Stirling Highway, Crawley, WA 6009, Australia.

E-mail: xuan.wu@unisa.edu.au; haolan.xu@unisa.edu.au

Numerical simulation: The numerical simulation was conducted by COMSOL Multiphysics 5.6 version. The modules of Chemical Species Transport and Laminar Flow were used for evaluating ion diffusion in the crystallizer, and presented as the distribution of ion concentrations in the crystallizer. The distribution of ion concentration was studied by solving the following equations:

$$R = \frac{\partial c}{\partial t} + \nabla \cdot J + u \cdot \nabla c$$

$$J = -D \nabla c$$

$$\rho \frac{\partial u}{\partial t} + \rho(u \cdot \nabla)u = \nabla \cdot [-pI + K]$$

$$\rho \nabla \cdot u = 0$$

Where R is the surface reaction of the ions; c and t present the concentration and time; J , u , I and K were the ion diffusion driven by concentration gradient, the velocity field, the constitutive relation coefficient and the fluid viscosity. ρ is the density of the fluid.

In this work, the model was set as 2 WTL-crystallizer as shown in Fig. S9. The size of the geometry model was the same as the experimental one, having a thickness of 2 mm for WTLs and 1 mm for the photothermal layer. The water entrance was set at the bottom of the inclined slice. Since there is no chemical reaction involved in solar evaporation of brine, R was set as 0. The ion concentration thus was determined by the velocity field and diffusive coefficient. The velocity field was driven by evaporation and the diffusive coefficient was a constant ($1.33 \times 10^{-9} \text{ m}^2 \text{ s}^{-1}$, corresponding to 7 wt% brine). The ion concentrations of the initial crystallizer and the brine were both set as 1256 mol m^{-3} (i.e., 7 wt% brine). The density of the brine was calculated and set as 1.049 g cm^{-3} . According to the experimental result, the simulated ion concentration was shown in Fig. 5b.

Salt crystallization evaluation: The salt mass harvest was calculated by the results of time-dependent evaporated mass change and ion concentration change using the following equations:

$$m_{total} = C_{initial} V_{initial}$$

$$m_{temporal} = C_{temporal} V_{temporal}$$

$$m_{salt\ harvest} = m_{total} - m_{temporal} = C_{initial} V_{initial} - C_{temporal} V_{temporal}$$

$$V_{temporal} = V_{initial} - V_{evaporated}$$

Where m_{total} , $m_{temporal}$ and $m_{salt\ harvest}$ represent the total salt mass, the salt mass dissolved in brine along with evaporation and the salt mass harvest through crystallization. $V_{initial}$,

$V_{temporal}$ and $V_{evaporated}$ are the initial volume of brine, the temporal volume of brine and the evaporated volume of brine during evaporation process.

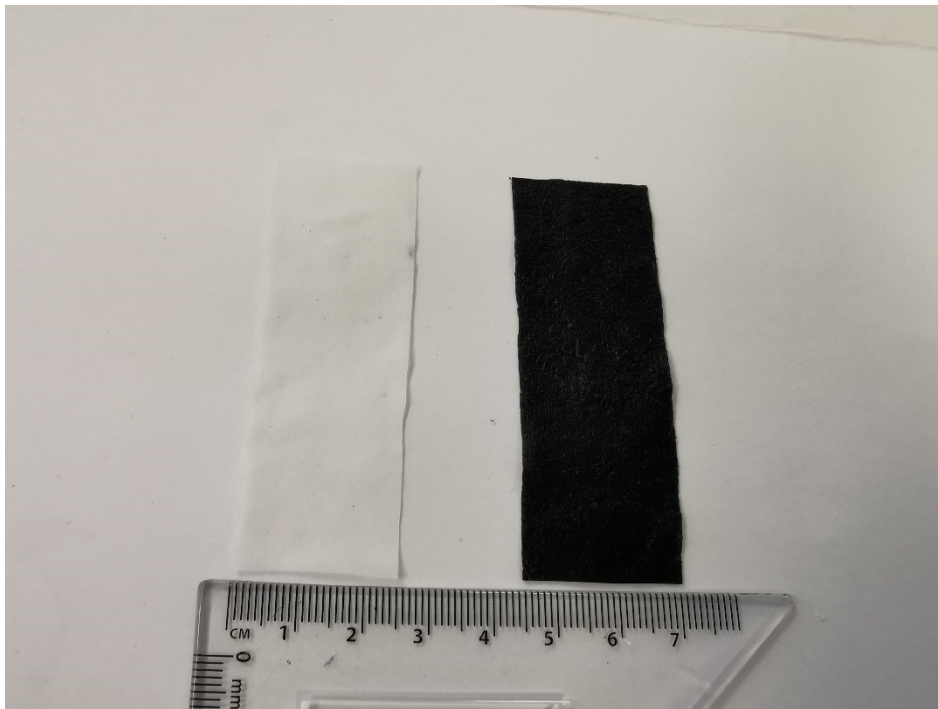


Fig. S1 Photograph of BFP before (left) and after (right) rGO coating

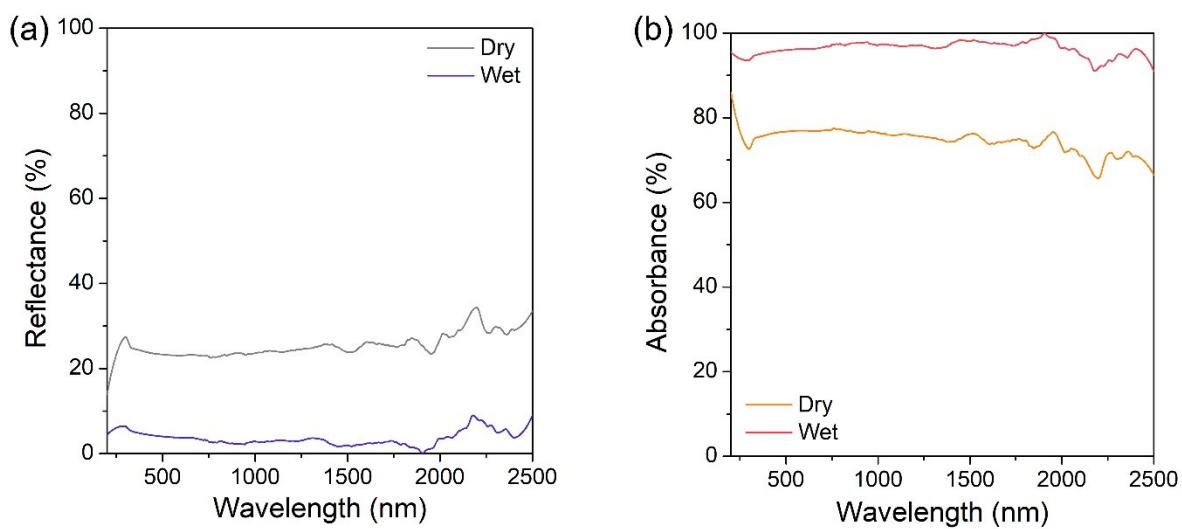


Fig. S2 Reflectance (a) and absorbance (b) spectra of the rGO-BFP in dry and wet state.

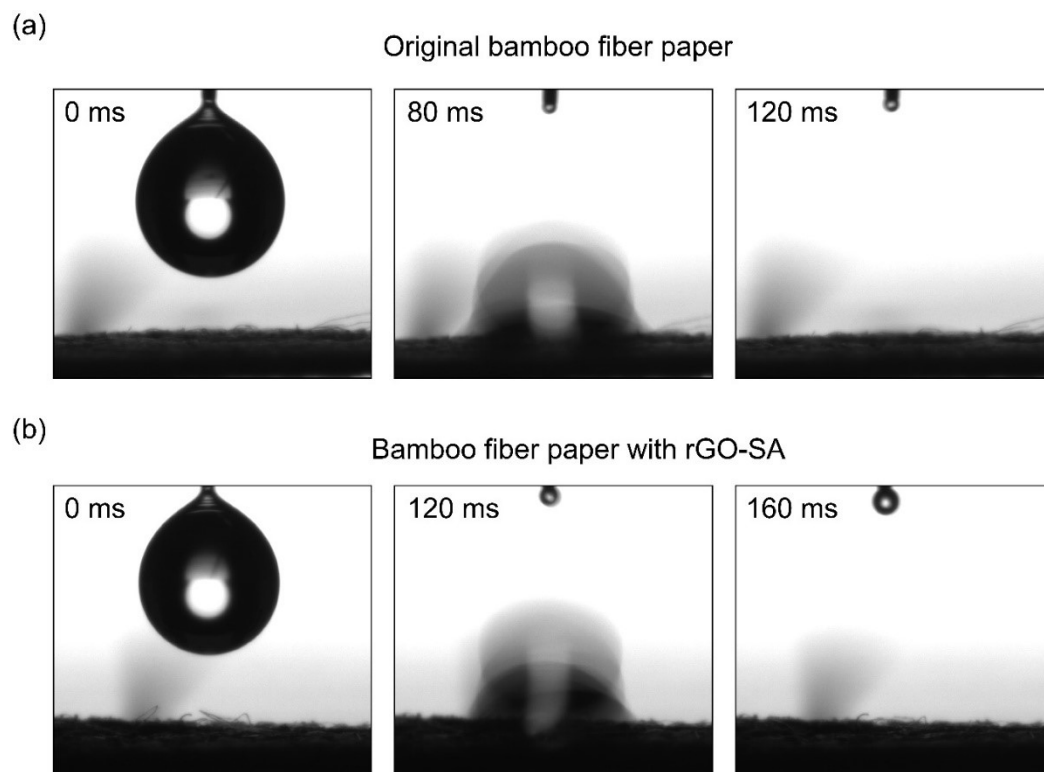


Fig. S3 Snapshots of absorption of a water droplet by BFP (a) and rGO-BFP (b).

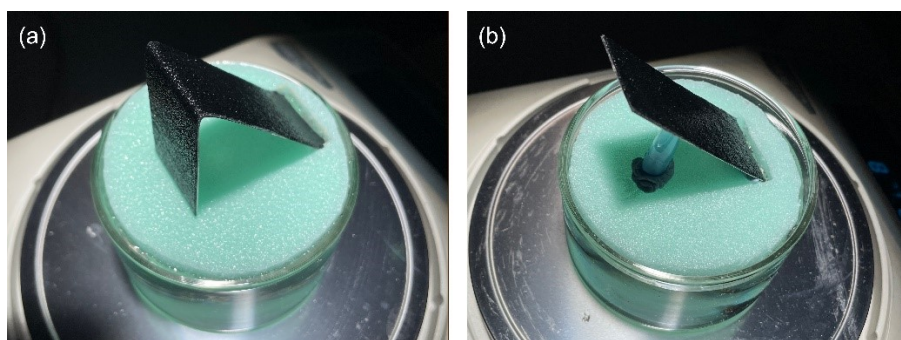


Fig. S4 Photographs of 45°-crystallizers with (a) and without (b) vertical slice.

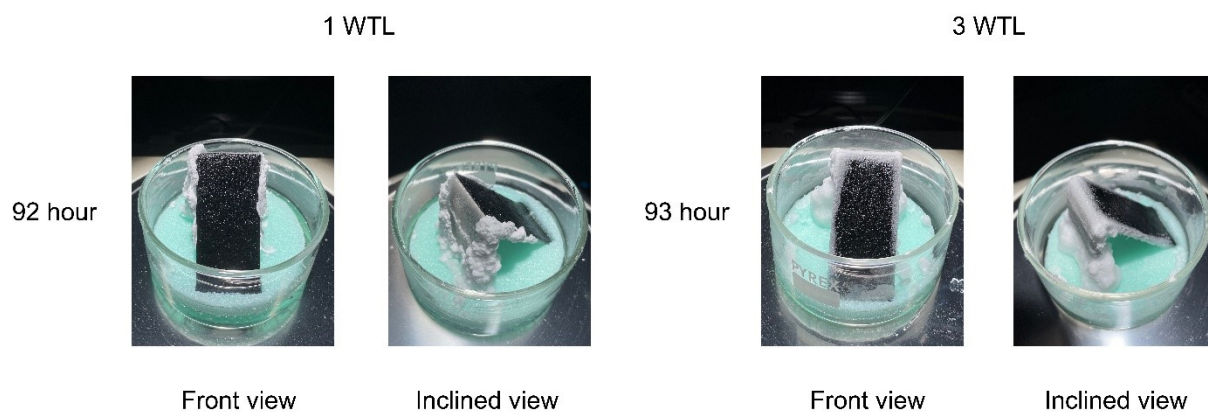


Fig. S5 Photographs of salt deposition on 1 and 3 WTL-crystallizers after fully water removal by solar evaporation.

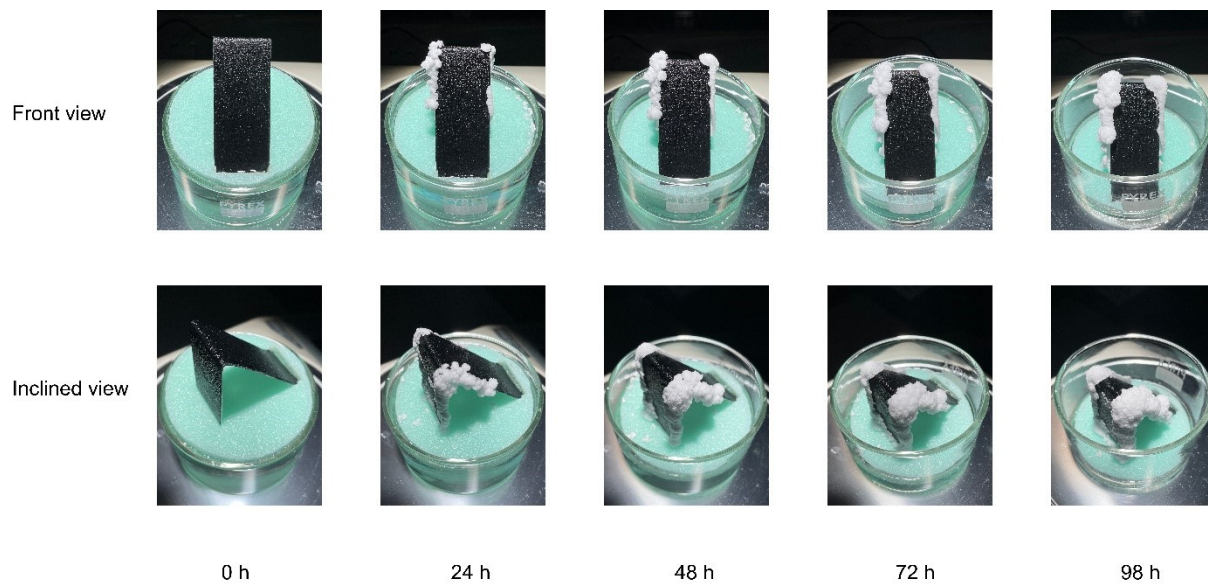


Fig. S6 Photographs of salt deposition on 0 WTL-crystallizer during solar evaporation.

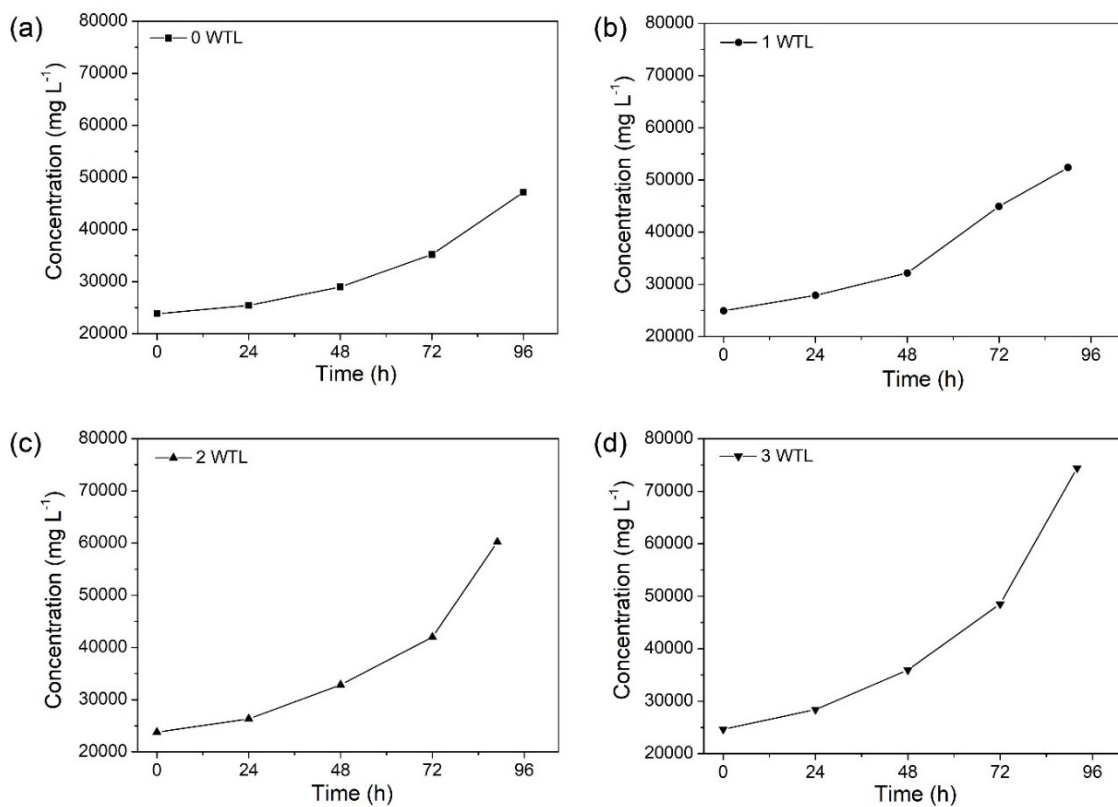


Fig. S7 (a-d) Concentration changes of Na^+ in the brine with 0, 1, 2 and 3 WTL-crystallizers during long-term solar evaporation.

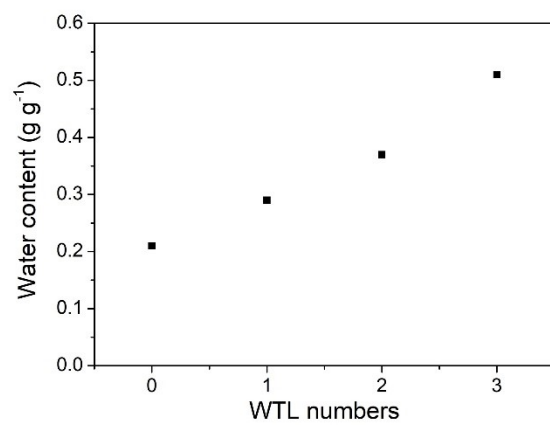


Fig. S8 Water content of the salts crystallized on 0, 1, 2 and 3 WTL-crystallizers.

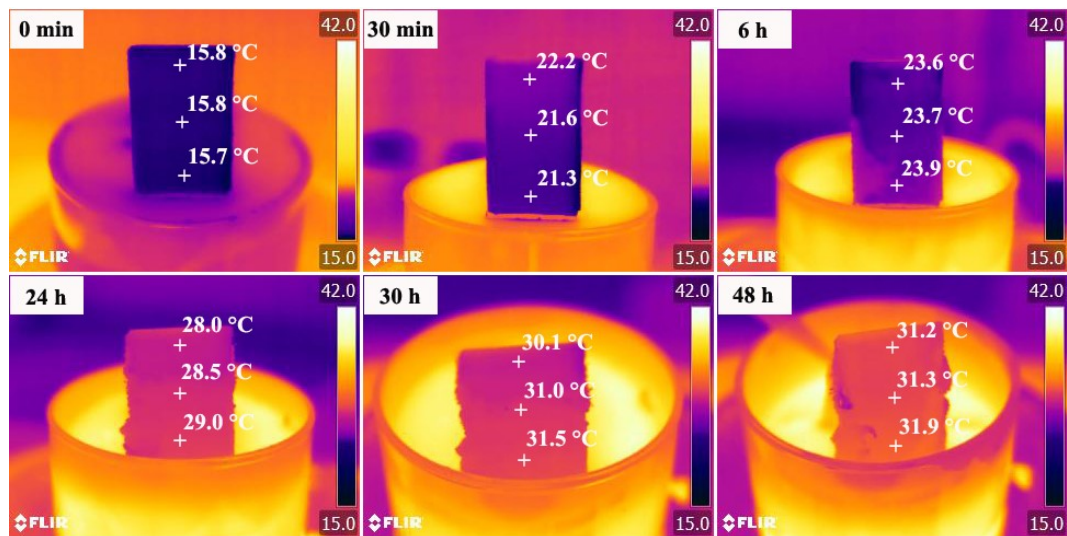


Fig. S9 IR images of the vertical slice of the 2WTL-crystallizer during solar evaporation process under one sun irradiation.

During the first 6 h brine evaporation, the average surface temperature of the vertical slice was lower than the environment temperature (25 ± 0.5 °C). Therefore, in this period the evaporator harvested energy from the surrounding environment. As the water evaporation progressed and salt gradually accumulated, the surface temperature of the vertical slice increased. In addition, the dropped water level placed the evaporation surface below the mouth of water container. The high-temperature environment inside the water container also led to the high surface temperature of the vertical slice. For example, after 24 hours, the surface temperature of the vertical slice was > 28 °C, slightly higher than the environment temperature. Therefore, there was energy loss from the vertical slice to the surrounding environment by radiation and convection.

Time	Radiation energy gain/loss (W)	Convection energy gain/loss (W)
30 min	0.021	0.038
6 th hour	0.008	0.014
24 th hour	-0.022	-0.037
30 th hour	-0.038	-0.065
48 th hour	-0.042	-0.072

Table S1 Calculated energy gain/loss of the vertical surface via radiation and convection at different solar evaporation stages. “-” means energy loss from vertical surface to the environment.

The energy exchange between the vertical slice and environment is calculated based on the following equations:

$$E_{\text{radiation}} = -A\varepsilon\sigma (T^4 - T_E^4)$$

$$E_{\text{convection}} = -Ah (T - T_E)$$

Where A is the evaporation surface area (11.25 cm²), T is the average temperature of the evaporation surface (K), T_E is the ambient temperature (25 °C), ε is emissivity of the absorbing surface (~0.95), σ is the Stefan–Boltzmann constant (5.67× 10⁻⁸ W m⁻² K⁻⁴), h is convection heat transfer coefficient (10 W m⁻² K⁻¹).

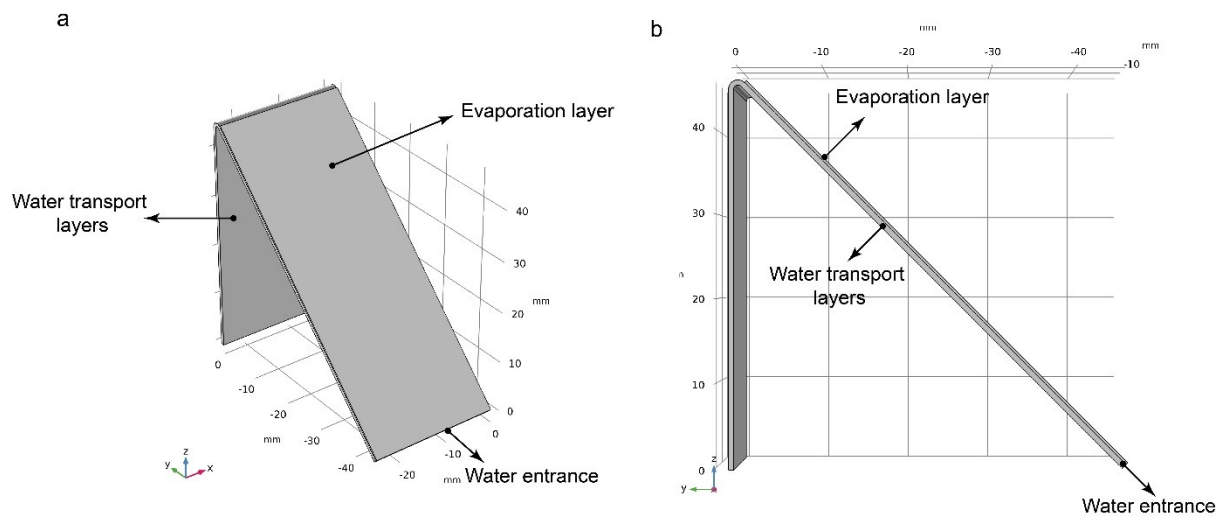


Fig. 10 Geometries of the model 2 WTL-crystallizer for numerical simulation in inclined view (a) and side view (b).